Optical Materials 32 (2010) 827–831

Contents lists available at ScienceDirect

Optical Materials

journal homepage: www.elsevier.com/locate/optmat

Europium doped zirconia luminescence

Krisjanis Smits [a,*], Larisa Grigorjeva [a], Donats Millers [a], Anatolijs Sarakovskis [a], Agnieszka Opalinska [b], Janusz D. Fidelus [b], Witold Lojkowski [b]

[a] Institute of Solid State Physics, University of Latvia, Riga, Latvia
[b] Research Institute of High Pressure Physics, Warsaw, Poland

ARTICLE INFO

Article history:
Received 6 October 2009
Received in revised form 2 March 2010
Accepted 3 March 2010
Available online 3 April 2010

Keywords:
Zirconia
Luminescence
Eu^{3+}
Crystalline structure

ABSTRACT

The luminescence properties and crystalline structure of ZrO_2:Eu nanocrystals doped with different concentrations of Eu were studied. Luminescence from the Eu^{2+} state was not observed even if the electrons and holes were created up to $\sim 10^{19}$ cm^{-3}; thus it was suggested the Eu^{3+} was not an efficient trap for electrons possibly due to Eu^{3+} negative charge relative to the crystalline lattice. The mutual interaction between Eu^{3+} ions was not strong up to 5 at.% concentration. The stabilization of ZrO_2 tetragonal as well as cubic structure by Eu^{3+} is possible.

1. Introduction

Zirconia (ZrO_2) is an outstanding material for use in optics – due to its wide band-gap the material has good transparency, the refractive index and hardness of material are also high [1]. On the other hand, the phonon energy of the ZrO_2 is low and therefore the luminescence thermal quenching is less efficient than in some other optical materials.

The luminescence of ZrO_2 doped with rare earth (RE) ions has been studied by a number of researchers [2–5]. The luminescence of Eu^{3+} is sensitive to the ion surrounding symmetry; therefore this luminescence is a probe for the crystal structure. The ZrO_2 has three polymorphs – monoclinic, tetragonal and cubic. Only the monoclinic phase of undoped ZrO_2 is stable at RT; the tetragonal and cubic phases are not. However, by incorporation of divalent and trivalent cationic species such as Mg^{2+}, Ca^{2+}, Y^{3+}, stable tetragonal and cubic phase of ZrO_2 at RT have been prepared [6]. The oxygen vacancies incorporated for charge compensation were suggested to be the main agents for tetragonal and cubic structure stabilization [7]. Thus it is possible to study the luminescence of RE ions incorporated in different crystalline structures with the same chemical composition. The cationic species added to ZrO_2 for tetragonal and cubic phase stabilization (Mg, Ca, and Y) could affect the luminescence of RE ions. The RE ions substitutes Zr^{4+} ions in ZrO_2 and since the RE ion is inovalent (the charge state 2+ or 3+), the oxygen vacancy is involved for charge compensation. Therefore it is expected that the ZrO_2 doped with Eu^{3+} could result in tetragonal and cubic phase stabilization.

The luminescence from transitions $^5D_0 \rightarrow {}^7F_1$ and $^5D_0 \rightarrow {}^7F_2$ is most intense for the Eu^{3+} ion and the corresponding luminescence bands in ZrO_2 have been described and discussed by several authors. The luminescence of the Eu^{3+} ion in ZrO_2:N was studied by Gutzov and Lerch [8] and differences in Eu emission and excitation were observed for different crystalline structures of ZrO_2; however the low intensity of luminescence did not allow high enough spectral resolution for ascertaining details. The Quan et al. [9] described results of luminescence ZrO_2:Eu synthesized by a spray pyrolysis and surmised that incorporation of Eu ions up to 10% did not change ZrO_2 structure. Contrary to this finding the ZrO_2 nanocrystal tetragonal structure stabilization by Eu^{3+} ions was observed [10,11]. The splitting of Eu^{3+} luminescence bands in ZrO_2:Eu was observed [12] after a thermal treatment of the sample. The origin of splitting observed was supposed to be due to the ground state spin–orbit splitting and interaction with crystalline field. The difference in ZrO_2:Eu luminescence bands positions was observed for tetragonal and cubic phase samples [13,14]. The study of luminescence from ZrO_2:Eu tetragonal phase [15] revealed that the luminescence band corresponding to $^5D_0 \rightarrow {}^7F_2$ transition was centred at 604 nm; the other observed band at 613 nm was ascribed to a defect perturbed state. Thus the results of ZrO_2:Eu luminescence study are different, some of them contradict to each other. Since it is known that luminescence of other RE ions depend on the ZrO_2 crystalline structure (e.g. [3]) and the ZrO_2 tetragonal as well as the cubic structure can be stabilized by incorporation of RE ions [4], the study of ZrO_2 nanocrystals doped with different

* Corresponding author. Tel.: +371 26538386.
E-mail address: smits@cfi.lu.lv (K. Smits).

0925-3467/$ - see front matter © 2010 Elsevier B.V. All rights reserved.
doi:10.1016/j.optmat.2010.03.002

concentration of Eu^{3+} ions was carried out – to attempt to clarity the differences observed in the previous studies.

2. Experimental

2.1. Samples

The ZrO_2 nanocrystals, both Eu^{3+} doped (Eu content from 0.1 at.% up to 5 at.%) and yttrium stabilized (Y content 6 at.%) Eu (0.05 at.%) doped, were used in experiments. An additional sample containing 10 at.% Eu was prepared for ascertaining the possibility of ZrO_2 cubic structure stabilization. The nanocrystals were produced by the microwave driven hydrothermal method described in details by Lojkowski et al. [16]. The grain size of nanocrystals was within 30–40 nm (determined by the BET method) for all samples after annealing at 750 °C. The energy dispersive X-ray analysis of samples using equipment Eagle III XPL was prepared for the content control of Eu and some unexpected impurities. The crystalline structure of samples was checked by XRD using the X-ray Diffractometer X'Pert Pro MPD.

2.2. Optical measurements

The measurements of luminescence and FT-IR absorption were carried out at RT. The measurements of luminescence were prepared using three different excitation sources: (I) YAG laser FQSS266 (CryLas GmbH) 4th harmonic, 266 nm (4.66 eV), 2 ns pulses; (II) pulsed electron beam, 270 keV acceleration voltage, flux 4×10^{12} el/cm^2, 10 ns pulses; (III) optical parametric oscillator (OPO) of type NT342/3UV (EXPLA). The samples for luminescent measurements were lightly pressed into small stainless-steel cells, all the cells have strongly the same size and thus the comparison of luminescence intensities from the samples was possible. The luminescence spectra were recorded using the Andor Shamrock B-303i spectrograph (spectral resolution ~0.1 nm) equipped with a CCD camera (Andor DU-401A-BV) at exit port. The equipment has the capability to record spectra using a variable width time gate at the different delay relative to excitation pulse. Therefore the luminescence spectra at different delay times were recorded. The decay kinetics of luminescence were measured using a photon counting head H8259-02 (HAMAMATSU) and a P7887 counting board (Fast ComTec GmbH) with minimal time bin 0.25 ns. The time resolution of the system was 2 ns without using the deconvolution and it was limited by descending part of excitation pulse. The monochromator MDR-2 (LOMO, Russia) and PMT were used for the registration of luminescence excited by a pulsed electron beam. The output signal from PMT was displayed on the digital oscilloscope TDS 5052B (TEKTRONIX). The time resolution of this registration system was 12 ns.

The ZrO_2:Eu nanocrystalline powder was dispersed in the potassium bromine powder and the pellets were pressed from this powder mixture for IR measurements. The IR absorption spectra of pellets were measured using the FT-IR spectrograph EQUINOX 55 (Bruker GmbH).

3. Results and discussion

The actual content of Eu in the samples was estimated with energy dispersive X-ray analysis. Results for samples studied were collected in Table 1. These results showed that the main dopant is Eu in ZrO_2:Eu nanocrystals and the content of unexpected impurities is significantly less than that of Eu. The exception was Y stabilized sample – in this sample the Y content was much larger than that of Eu.

Table 1
The Eu content in the samples.

Composition	Eu (at.%)	Y (at.%)	Mentioned in the text as
ZrO_2:Eu_2O_3	0.19	0	ZrO_2:Eu containing 0.1% Eu
ZrO_2:Eu_2O_3	0.51	0	ZrO_2:Eu containing 0.5% Eu
ZrO_2:Eu_2O_3	0.72	0	
ZrO_2:Eu_2O_3	1.06	0	
ZrO_2:Eu_2O_3	1.75	0	
ZrO_2:Eu_2O_3	4.54	0	ZrO_2:Eu containing 5% Eu
ZrO_2:Eu_2O_3	10	0	ZrO_2:Eu containing 10% Eu
ZrO_2:Y_2O_3:Eu_2O_3	0.05	6	Y stabilized ZrO_2Eu containing 0.05% Eu

The incorporation of Eu^{3+} in ZrO_2 is expected; however, under some kind of excitation the electron could be trapped by Eu^{3+} and anticipate that the Eu^{2+} excited state was formed. Since it is well known that the Eu^{2+} luminescence is within 390–520 nm range this region was monitored under two kinds of excitation: (I) selective using OPO for the excitation scanning within 220–300 nm with the step 1 nm; (II) non-selective using electron beam pulses. The second kind of excitation led to the creation of electrons and holes, the estimated density of charge carriers was close to 10^{19} cm^{-3}. The range of expected Eu^{2+} luminescence overlaps with ZrO_2 intrinsic defects luminescence. These two kinds of luminescence can be separated using the time resolved technique since the Eu^{2+} luminescence decay is within microseconds [17,18], whereas ZrO_2 luminescence decay does not exceed 50 ns [19]. The luminescence of Eu^{2+} was not detected under both kinds of excitation even for sample containing 10 at.% Eu. It was concluded that the trapping of the electron by Eu^{3+} and formation of the Eu^{2+} excited state in ZrO_2:Eu is not efficient. This result coincides with conclusion made by Dorenbos [20] that the Eu^{2+} is never stable on trivalent RE site. The possible reason why the Eu^{2+} was not formed in the ZrO_2 is that the Eu^{3+} has a negative charge relative to the ZrO_2 lattice and therefore the probability of electron trapping could be negligible. The luminescence of the ZrO_2 intrinsic defects as well as Eu^{3+} was observed in our experiments under both kinds of excitation. The YAG laser was used for excitation in the experiments described below carried out for the study of ZrO_2:Eu containing different amounts of Eu.

The charge transfer band of ZrO_2:Eu peaks within a 240–250 nm range [21] and a long wave tail of this band extends until 280 nm. Therefore the YAG laser 4th harmonic (266 nm or 4.66 eV) excited the Eu luminescence via charge transfer process. The luminescence spectra shown in Fig. 1a curve (1) were recorded within a 32 ns time gate without delay and curve (2) with 32 ns delay relative to the excitation pulse for the sample containing the Eu of (5 at.%).

The luminescence spectrum recorded without any delay showed one broad luminescence band peaking at ~445 nm. This band is due to the ZrO_2 intrinsic defects and the decay of this luminescence was fast – after 32 ns delay this band was not detectable (Fig. 1a). The luminescence band position and its decay time correspond to intrinsic defects (related to oxygen vacancies) luminescence. The enhancement of Eu concentration led to the suppression of intrinsic defects luminescence. The peculiarities of the intrinsic defects luminescence were discussed elsewhere [22]. The weak intensity and poor resolved luminescence bands in the delayed spectrum (in the oval in Fig. 1a) were from Eu^{3+} ions. The bands mentioned were due to $^5D_0 \rightarrow 7F_j$ (j = 1, 2, 3) transitions, all to be partially forbidden; therefore the decay time of this luminescence was relative long and the spectrum could be recorded using the wide time gate (32 μs), thus improve the noise to signal relation and get a better spectral resolution (Fig. 1b). The more intense bands correspond to the $^5D_0 \rightarrow {}^7F_1$ (magnetic dipole) and $^5D_0 \rightarrow {}^7F_2$ (electric dipole) transitions, corresponding bands usually

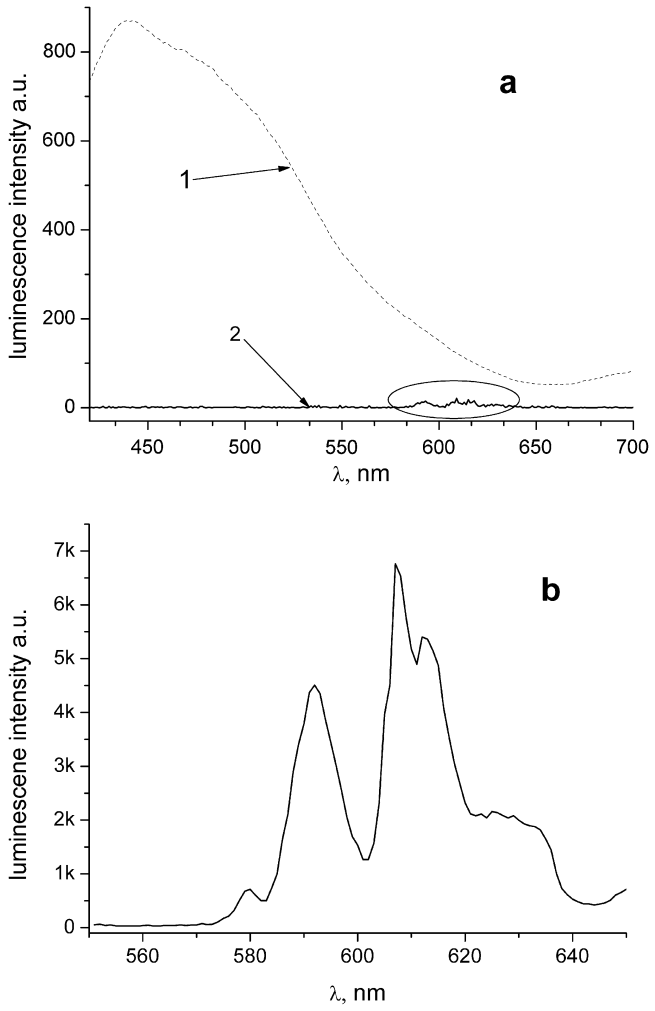

Fig. 1. Luminescence spectra of ZrO_2:Eu 5 at.%. (a) Recorded within 32 ns time gate, 1 – without delay, 2 – at 32 ns delay relative o excitation pulse; (b) 32 ns delay relative to the excitation pulse recorded within 32 ms gate.

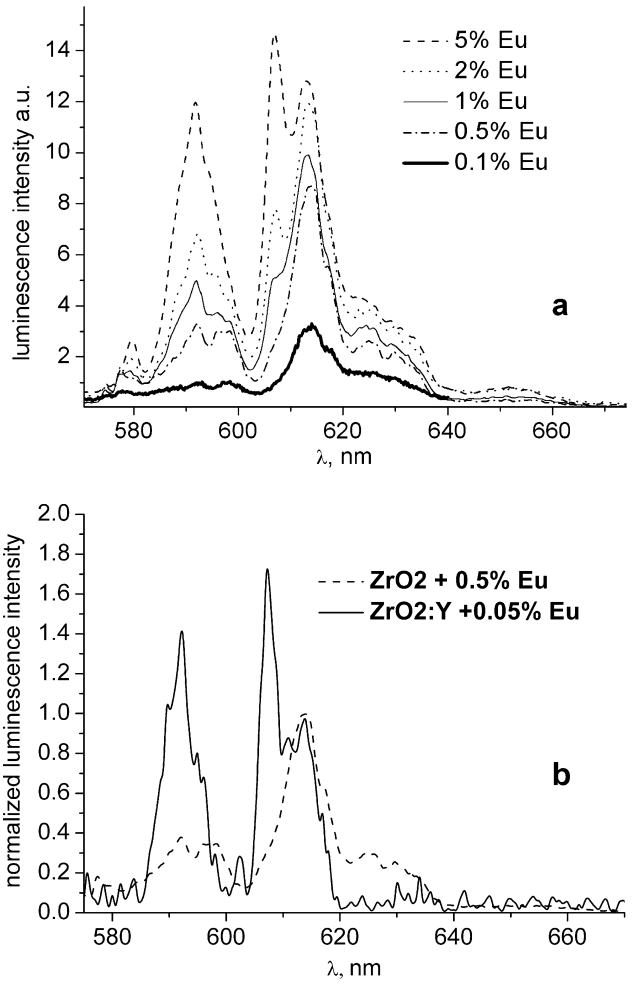

Fig. 2. Luminescence spectra of ZrO_2 containing different concentration of Eu; (a) the band peaking at 607 nm was resolved for samples containing Eu above 1 at.%; (b) the luminescence spectrum of Y stabilized ZrO_2Eu containing 0.05% Eu, the luminescence band peaking at 607 nm is dominant.

peaks at 570–600 nm and 600–640 nm. The much weaker luminescence comes from $^5D_0 \rightarrow {}^7F_3$ transitions peaking at 640–660 nm region The luminescence from $^5D_0 \rightarrow {}^7F_2$ transition in monoclinic ZrO_2 split in three bands, these bands is associated with lower local symmetry of Eu^{3+} [12]. In order to ascertain the luminescence intensity dependence on the Eu^{3+} concentration, the intensity of luminescence at 614 nm (measurements at 614 nm instead of 613 was made to reduce overlapping from 607 band) was measured for ZrO_2:Eu samples with different Eu contents within the range of 0.1–5 at.% (Fig. 2a). Similar luminescence intensity dependence from Eu concentration is for bands 620–640 nm, because these bands have the same origin as for band peaking at 613 nm. The luminescence intensity measured at this wavelengths tend to saturate above 2 at.% (Fig. 3).

However, the luminescence spectra for these samples were different – for samples containing Eu above 1 at.% the additional luminescence band centred at 607 nm appears (Fig. 2a). A similar band peaking within 605–607 nm range was described in [9,12,23] where it was also concluded that this band corresponds to the $^5D_0 \rightarrow 7F_2$ transition. The intensity of this band became most intense at Eu content of 5 at.% (Fig. 2a).

Therefore it was assumed that better characteristic for the luminescence intensity dependence on concentration can be the light sum of $^5D_0 \rightarrow {}^7F_2$ transitions peaks in different surroundings. This light sum is proportional to the area under 607 and 613 nm bands. The area was determined as an integral of spectrum over 600–640 nm range. This integral intensity of luminescence did not showed saturation even up to 5 at.% of Eu content (Fig. 3) indicating that the mutual interaction between Eu^{3+} ions in ZrO_2 is week and the concentration quenching of luminescence was not noticeable for this concentration. The concentration quenching is expected to be at ~10 at.% Eu. The two luminescence bands for the same electron transition in Eu^{3+} is evidence that ion was incorporated in two different symmetry sites. The probability of $^5D_0 \rightarrow {}^7F_2$ (electric dipole) transition strongly depends on the Eu^{3+} surrounding symmetry, whereas probability of $^5D_0 \rightarrow {}^7F_1$ (magnetic dipole) transition is nearly independent of the Eu^{3+} surrounding symmetry. Therefore the relation of luminescence intensities of corresponding bands ($I_{el.dip.}/I_{magn.dip.}$) is the Eu^{3+} surrounding symmetry characteristics. This relation is known as the asymmetry ratio [13] and the larger asymmetry ratio is for lower surrounding symmetry of Eu^{3+}. The values was estimated calculating integral light sum from 570 to 600 nm for magnetic dipole transition and light sum from 600 to 640 nm for electric dipole transition, the asymmetry ratio are 2.7 and 2.2 for samples containing 0.1 and 5 at.% Eu respectively. Hence, the Eu^{3+} surrounding symmetry was higher for sample containing 5 at.% Eu, than in sample doped with 0.1 at.% Eu. The asymmetry ratio of this sample was compared with that for the Y stabilized and the Eu doped tetragonal phase $Zr_{0.94}Y_{0.06}O_2$:Eu nanocrystals containing 0.05 at.% Eu. The lumines-

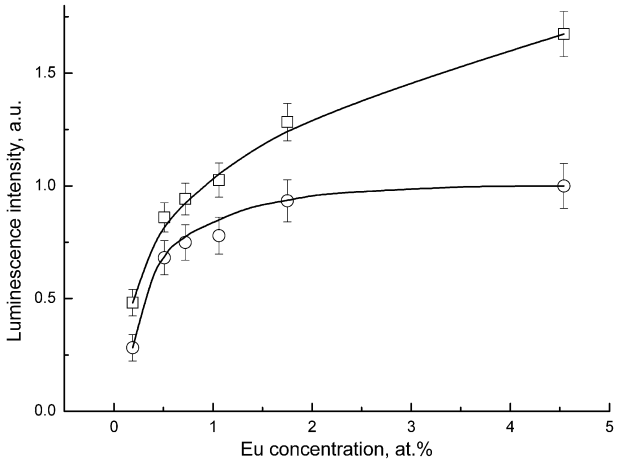

Fig. 3. Luminescence intensity dependence on Eu concentration, open circles – intensity of 613 nm band, open squares – integral intensity within range 600–640 nm, the scale for integral intensity was reduced.

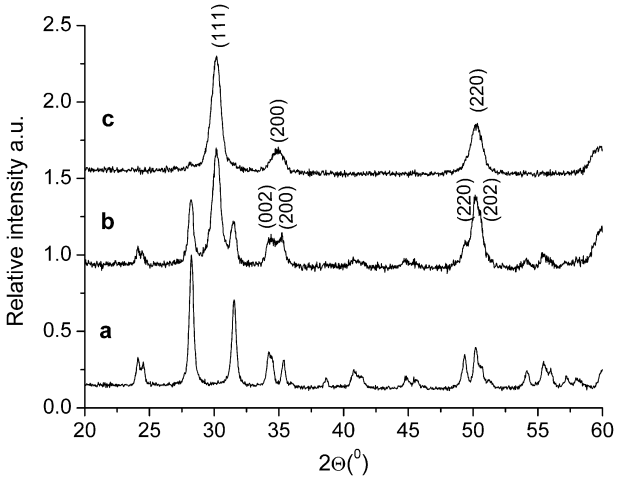

Fig. 5. XRD patterns for samples ZrO_2:Eu containing 0.1 at.% Eu (sample with dominant monoclinic phase); 5 at.% Eu (tetragonal with admixture of monoclinic sample); 10 at.% Eu (sample with dominant cubic phase).

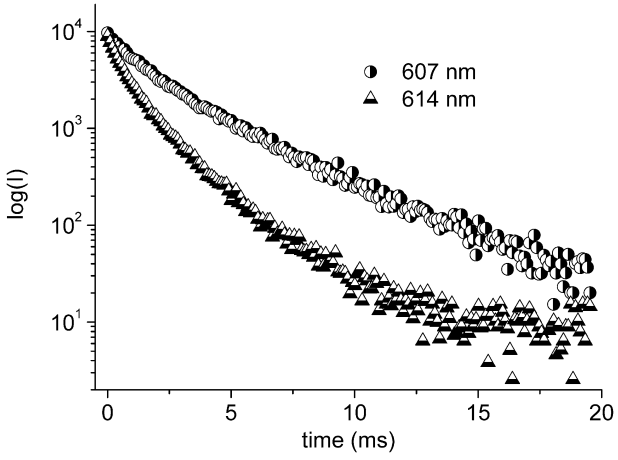

Fig. 4. Luminescence decay kinetics for sample with 5 at.% Eu, the decay of 607 nm band is slower.

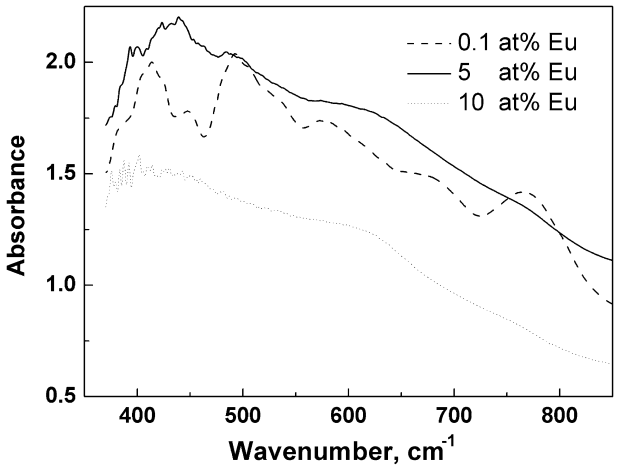

Fig. 6. The FT-IR absorption spectra for samples ZrO_2:Eu containing 0.1; 0.5 and 10 at.% Eu.

cence spectrum of this sample is in Fig. 3b and the estimated asymmetry factor is 1.3. Another parameter sensitive to the symmetry is Eu^{3+} luminescence decay time. Luminescence decay measured in the band peaking at 607 nm was slower than for 613 nm band (Fig. 4). This is additional evidence that the Eu^{3+} surrounding symmetry is higher for the sample containing 5 at.% Eu.

Therefore from the results it is suggested that the symmetry is higher for heavily doped ZrO_2:Eu nanocrystals, because these nanocrystals have the tetragonal or even cubic crystalline structure. This suggestion was checked by XRD analysis. The XRD patterns (Fig. 5) clearly showed that the sample containing 0.1 at.% Eu was monoclinic and the sample containing 5 at.% Eu was a mixture from tetragonal and monoclinic phase nanocrystals.

The conclusion ascertained that both luminescence bands – at 613 nm and at 607 nm correspond to $^5D_0 \rightarrow {}^7F_2$ transition in Eu^{3+} ion, the first one in the monoclinic phase and the second one in the tetragonal and also cubic phase ZrO_2:Eu nanocrystals. This result is in agreement with that described in [13]. The results of XRD experiments shows that the Eu^{3+} can stabilize the ZrO_2 tetragonal and cubic phases. The XRD for the sample containing large amounts (10 at.%) of Eu was quite similar to that for the sample (5 at.%) with ZrO_2 monoclinic and tetragonal phase mixture (Fig. 5). It should be noted that the XRD reflex peaks of the tetragonal and cubic phase ZrO_2 seems similar, however some differences are present. The peak position and peak intensities for tetragonal and cubic phase ZrO_2 differs, therefore it is possible to estimate, that the ZrO_2:Eu sample containing 10 at.% Eu (Fig. 5) is cubic, and Eu stabilizes ZrO_2 cubic phase. The etalons with references 01-080-2155 and 01-081-1551 [24] were used to determine the tetragonal and cubic phases.

It is known the phonon energies are different for monoclinic, tetragonal and cubic phase ZrO_2 and that the IR absorption spectra are different also, however the bands in IR spectra for tetragonal and cubic phase ZrO_2 were poor resolved [23]. The IR absorption spectra were displayed in Fig. 6 for the three ZrO_2:Eu samples containing 0.1 at.% (monoclinic), 5 at.% (tetragonal) and 10 at.% Eu. The spectrum of monoclinic phase ZrO_2:Eu showed four absorption bands at 418, 505, 575 and 754 cm^{-1}. The tetragonal phase ZrO_2 spectrum reveals two broad and poor resolved absorption bands at 459 and 470 cm^{-1} [23], in the spectrum of the sample ZrO_2:Eu containing 5 at.% Eu we cannot bring out these bands clearly. An additional band at ~600 cm^{-1} indicates that admixture of cubic phase is possible, however the XRD data indicate that tetragonal phase is. The sample containing 10 at.% Eu showed similar to that for 5 at% Eu – one very broad band extending within 400–750 cm^{-1}

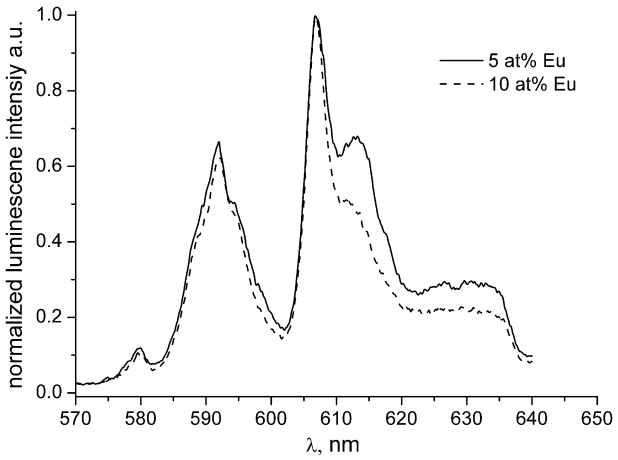

Fig. 7. The comparison of cubic and tetragonal structure ZrO_2:Eu luminescence spectra. Band peaking at 607 nm coincide in the both spectra.

and peaking at ~600 cm^{-1}. The absorption spectra shapes are similar to those described in [23] and the FT-IR spectrum of sample containing 10 at.% Eu corresponds well to the cubic phase ZrO_2. The luminescence spectrum of this sample is at Fig. 7, the band corresponding to the $^5D_0 \rightarrow {}^7F_2$ transition in Eu^{3+} ion peaks at 607 nm.

Thus the luminescence spectrum is similar to that of tetragonal structure sample. The similarity of Eu^{3+} luminescence in tetragonal and cubic phase ZrO_2 could be not exception since the same was observed for Dy^{3+} ion by Fu et al. [25]. The luminescence band peaking at 607 nm was observed in the ZrO_2:Eu cubic structure thin films [26] also. Therefore, it is possible that the Eu^{3+} luminescence spectra were similar for both tetragonal and cubic ZrO_2 structures. Hence, the Eu^{3+} is a luminescence centre and can stabilize the tetragonal as well as the cubic structure of ZrO_2. The stabilization of the cubic structure will be of interest since it is generally known that cubic structure nano- and micro-crystals are the most appropriate for the transparent ceramics sintering. Therefore, the cubic structure ZrO_2:Eu nanocrystals could be a raw material for making the transparent ceramics with efficient luminescence properties.

4. Conclusions

The Eu in ZrO_2 incorporates in the trivalent state; the luminescence of Eu^{2+} was not observed even under powerful pulsed electron beam irradiation. The luminescence integral intensity dependence on Eu concentration showed that mutual interaction between the Eu^{3+} ions is weak in ZrO_2 nanocrystals up to a 5 at.% concentration where the aggregation of dopant ions did not take place. The position of a luminescence band corresponding to the $^5D_0 \rightarrow {}^7F_2$ transition in the Eu^{3+} ion peaks at ~613 nm for the monoclinic phase and ~607 nm for the tetragonal and cubic phase ZrO_2. The monoclinic phase ZrO_2:Eu nanocrystals were dominant up to 1 at.% dopant concentration, at larger concentrations there is a tetragonal phase nanocrystals admixture. The XRD data and FT-IR spectra are strong evidences that Eu^{3+} ion change structure of ZrO_2 nanocrystals; at the same time the Eu^{3+} ion is also the luminescence centre and with structural changes the luminescence spectra changes. High concentration of Eu leads to stabilization of cubic phase of nanocrystalline ZrO_2, prepared by microwave driven hydrothermal method.

Acknowledgements

The work was partially supported by the Latvian National Material Research Programme, Latvian Council of Science Grants 09.1126 and 05.0026. One of us (K. Smits) was supported by ESF. The authors are grateful to Dr. A. Mishnov and Dr. L. Skuja for XRD data and energy dispersive X-ray analysis of samples.

References

[1] H.D.E. Harrison, N.T. McLamed, E.C. Subarao, J. Electrochem. Soc. 110 (1962) 23.
[2] G. Cabello, L. Lillo, C. Caro, G.E. Buono-Core, B. Chornic, M.A. Soto, J. Noncryst. Solids 354 (2008) 3919.
[3] H. Zhang, X. Fu, S. Niu, Q. Xin, J. Noncryst. Solids 354 (2008) 1559.
[4] J. Kaspar, P. Fornasiero, G. Balducci, R. Di Monte, H. Hickey, V. Sergo, Inorg. Chim. Acta 349 (2003) 217.
[5] H. Zhang, X. Fu, S. Niu, Q. Xin, Mater. Sci. Eng. 129 (2006) 14.
[6] R.C. Gavie, J. Phys. Chem. 82 (1978) 218.
[7] S. Fabris, A.T. Paxton, M.W. Finnis, Acta Mater. 20 (2002) 5171.
[8] S. Gutzov, M. Lerch, Opt. Mater. 24 (2003) 547.
[9] Z.W. Quan, L.S. Wang, J. Lin, Mater. Res. Bull. 40 (2005) 810.
[10] P. Salas, N. Nava, C. Angeles-Chavez, E. De la Rosa, L.A. Diaz-Torres, J. Nanosci. Nanotechnol. 8 (2008) 6431.
[11] A. Mondal, S. Ram, J. Am. Ceram. Soc. 91 (2007) 329.
[12] L. Chen, Y. Liu, Y. Li, J. Alloys Compd. 381 (2004) 266.
[13] Huang-Qing Liu, Ling-Ling Wang, Shu-Guang Chen, Bing-Suo Zou, J. Alloys Compd. 1–2 (2008) 336.
[14] H. Zhang, H. Fu, S. Niu, G. Sun, Q. Xin, Mater. Chem. Phys. 91 (2005) 361.
[15] Liu Huangqing, Wang Lingling, Chen Shuguang, Zou Biugsuo, Peng Zhiwei, Appl. Surf. Sci. 253 (2007) 3872.
[16] A. Opalinska, C. Leonelli, W. Lojkowski, R. Pielaszek, E. Grzanka, T. Chudoba, H. Matysiak, T. Wejrzanowski, K.J. Kurzydlowski, J. Nanomater. (2006) 98769.
[17] M. Itoh, T. Sakurai, T. Yamakami, J. Fu, J. Lumin. 112 (2005) 161.
[18] F. Meister, Mbatenschuk, S. Droscher, A. Osvet, A. Stiegelschmitt, M. Weidner, A. Winnacker, Radiat. Meas. 42 (2007) 771.
[19] K. Smits, L. Grigorjeva, D. Millers, J.D. Fidelus, W. Lojkowski, IEEE Trans. Nucl. Sci. 55 (2008) 1523.
[20] P. Dorenbos, J. Lumin. 128 (2008) 578.
[21] E.F. Lopez, V.S. Escribano, M. Paniza, M.M. Camascialli, G. Busca, J. Mater. Chem. 11 (2001) 1891.
[22] K. Smits, L. Grigorjeva, W. Łojkowski, J.D. Fidelus, Phys. stat. Sol. (c) 4 (2007) 770.
[23] Shu Fen Wang, Feng Gu, Meng Kai Lu, Zhong Sen Yang, Guang Jun Zhou, Hai Ping Zhang, Juan Juan Zhou, Shu Mei Wang, Opt. Mater. 28 (2006) 1222.
[24] U. Martin, H. Boysen, F. Frey, Acta Cryst., Sec. B: Struct. Sci. 49 (1993) 403.
[25] Xiaoyan Fu, Shuyun Niu, Hongwu Zhang, Qin Xin, Mater. Sci. Eng. B 129 (2006) 14.
[26] K. Kuratani, M. Mizuhata, A. Kajinami, S. Deki, J. Alloys Compd. 408–412 (2006) 411.